# Fatigue Damage Evolution in Graded Materials

**F.Zeismann[1,*], M. Besel[1,a], A. Brueckner-Foit[1,b]**

[1]University of Kassel, Institute for Materials Engineering, Moenchebergstr. 3, 34125 Kassel

[*]zeismann@uni-kassel.de
phone / fax +49 (0)561 804-3696 / -3650

[a]m.besel@uni-kassel.de, [b]a.brueckner-foit@uni-kassel.de

***ABSTRACT.*** *The fatigue damage evolution of a thermo-mechanically graded material is investigated within the framework of an ongoing collaborative research center (SFB/TR TRR 30). The first results are presented which deal with the fatigue behavior of a flange shaft. The base material is a CrV-alloyed heat treatable steel in an engineering condition. The steel has a nearly fully pearlitic microstructure in the initial state, i.e. in an annealed condition. A martensite phase is formed in parts of the flange rod in the course of the thermo-mechanical treatment. The fatigue behavior of the different regions and their damage mechanisms leading to failure are identified. A procedure of determining the lifetime of the flange shaft is presented.*

## INTRODUCTION

This article deals with the fatigue behavior of low carbon steel in an engineering condition, i.e. steel with an inhomogeneous microstructure containing a lot of impurities, e.g. carbides and sulphides. Thermo-mechanical forming of round bars results in semi-fabricated products (flange shafts) with (geometrically) graded material properties due to a graded microstructure as a result of e.g. local martensite transformation [1]. The resulting multiphase structure consists of volumes containing ferrite/pearlite, a graded microstructure, and martensite. The aim of this ongoing research is the characterization of the fatigue behavior of these different microstructures, and the effect of their gradation on the fatigue behavior of the flange shaft during its later application.

Fig .1 shows a cross section of the flange shaft. The martensite phase corresponds to the dark areas in the cross section, whereas a ferrite/pearlite microstructure very similar to the original base material can be found in the light areas. The chemical composition of the material is given in Table 1. The round bars were locally heated up to 1300°C and held for 5s in order to trigger dissolving the carbides. The ensuing forming process

started with a certain degree of free forming followed by contact with a cooled die. The martensite transformation was brought about by contact with the cold die on the surface of the flange shaft and by contact of the unheated part of the original rod with the heated part in the course of the deformation process. The transition zone between the martensite and the base material is several millimeters wide and consists of a continuously changing microstructure.

More information on the local microstructure can be obtained by measuring the local hardness. Fig. 2 shows the results where the lighter colors are related to the softer phases.

Table 1. Chemical composition in wt.% of the low carbon steel

| C | Si | Mn | Cr | V | P | S |
|---|---|---|---|---|---|---|
| 0.47-0.55 | ≤ 0.40 | 0.70-1.10 | 0.90-1.20 | 0.10-0.25 | ≤0.035 | ≤0.035 |

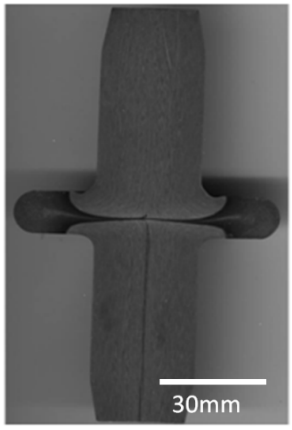


Figure 1. Flange shaft

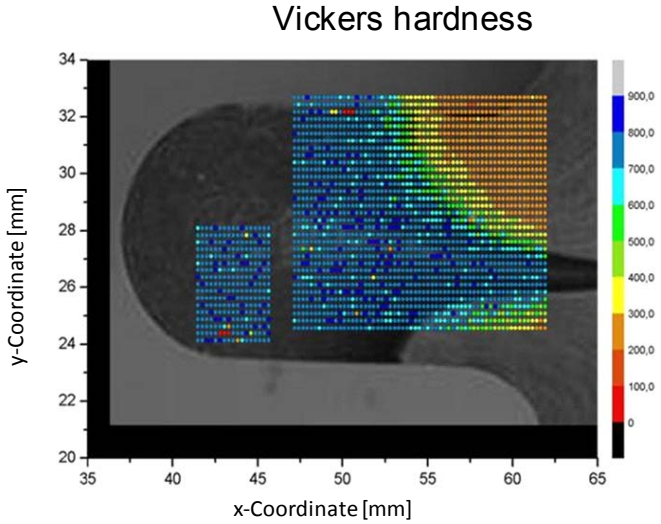


Figure 2. Estimated values of the Vickers hardness in the transformed area

## FATIGUE TESTS

Flat hourglass specimens were cut by spark erosion from the flange according to a well-defined cutting plan, s. Fig. 3.

Two types of specimens were used: continuously notched small specimens for fatigue tests and traditional fatigue specimens, s. Fig.3 and Fig. 4. All these specimens were ground and electro-polished.

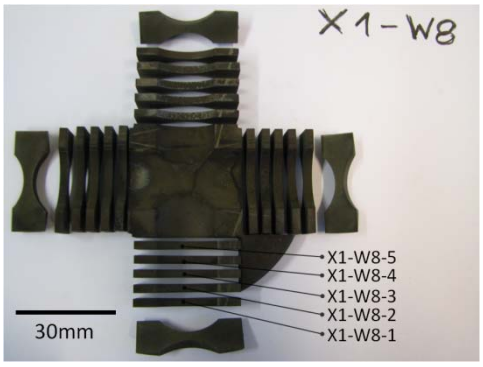


Figure 3. Fatigue Specimens (small) cut from the flange

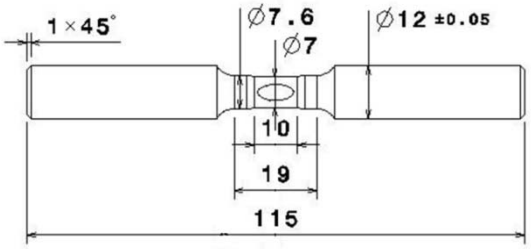


Figure 4. Traditional Fatigue Specimen

Comparison of Fig.1-2 and Fig.3 shows that the specimens with the last digit 1-4 (E2- E4 in Fig.5) were taken from the martensite area whereas specimens number"… -4" and "…-5" contained a mixture of microstructures ranging from base material to martensite. Hence it was possible to investigate both the tensile properties and the fatigue properties of the flange. In addition specimens were cut from the base material to study the mechanical behavior of the undeformed material. In this case round bars with flat notches were manufactured in addition to the small hourglass specimens described above.

Fig. 5 summarizes the result of load-controlled fatigue tests with R=-1. It can be seen that the life times of specimens taken from the transformed regions are much higher, and that there is not much difference between three outer locations in the flange. Moreover, the lifetimes in the transformed regions show a considerable amount of scatter.

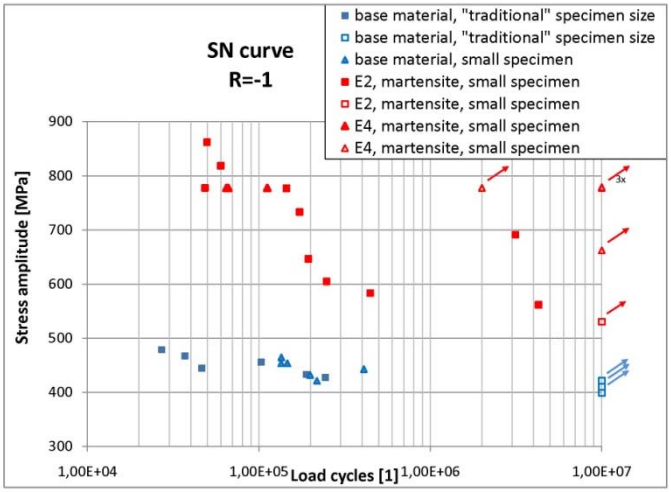


Figure 5. Fatigue life times of specimens cut from the flange

## DAMAGE ACCUMULATION PROCESS

There were three types of microscopic investigations of the damage accumulation process during fatigue loading

(i) The specimen surface was observed during the tests with a long range microscope [2]. Pictures were taken with a CCD camera and stored in a computer. This allowed scanning of the specimen surface and detecting microcracks shortly after initiation. Only selected specimens underwent this procedure because of the considerable experimental effort involved.

(ii) The specimen surface was photographed after failure with a digital microscope in order to determine the basic mechanisms of fatigue failure.

(iii) The fracture surfaces of failure specimens were observed in the SEM in order to find out the fatal flaw.

The ferritic-pearlitic phase (initial material state) shows a very complex damage evolution. Three different sites of crack initiation were identified for the base material. Crack initiation was found at sulphide inclusions, at pits, in the ferrite phase, and at its phase boundaries (ferrite/pearlite), respectively. Figure 6 shows an area of about 0.8x1.3 mm² of the damaged surface after 18,000 load cycles. The polished surface became rough due to local plastic deformation caused by the cyclic loading.

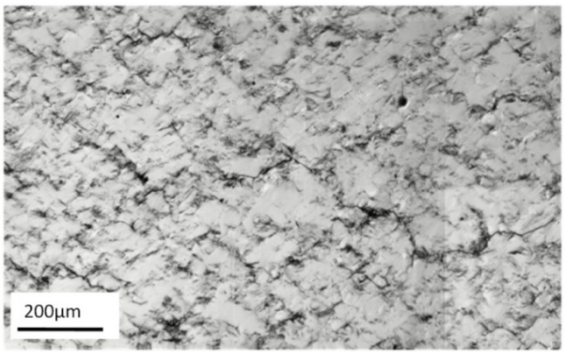


Figure 6. Extract of the surface scan taken after 18,000 load cycles

The whole surface of the specimen is covered with small microcracks and localized plastic deformation, respectively. On the basis of the pictures taken with the optical long distance microscope (e.g. Fig. 6) it is difficult to distinguish between microcracks and strong line-like plastic deformation due to the fact that both appear as black lines. But both of them represent an area of locally reduced material strength and therefore contribute to the damage state. As a result it is not necessary to distinguish clearly between localized line-like plastic deformations (which are potential cracks) and well-

defined cracks. This statement can be justified based on Figure 7. Although the etching took only 6 s, and afterwards the specimen was cleaned carefully, new small microcracks appeared immediately after etching in the areas of high plastic activity (see right picture of Fig.7).

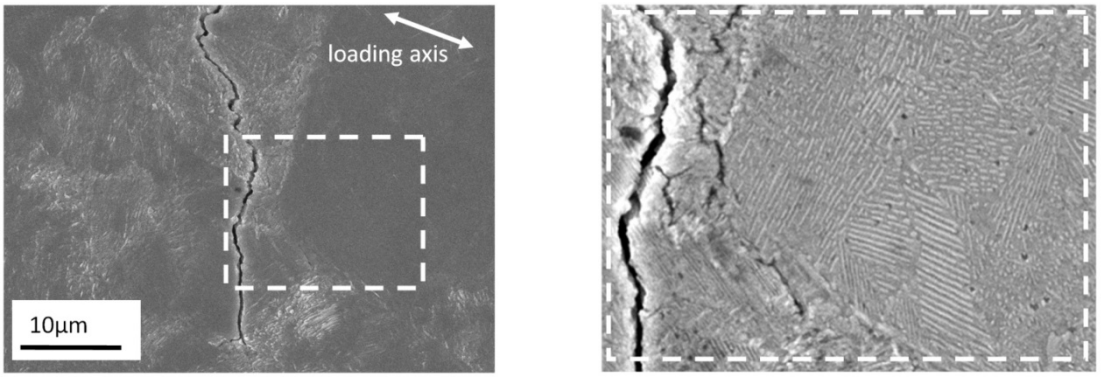


Figure 7. Pearlitic area with hardly any plastic deformation (right side: details of microstructure after etching)

Figure 7 illustrates the observation that most of the comparably large areas showing hardly any or no plastic deformation (Fig.6) correspond to fully pearlitic zones with comparably small spacing between the cementite lamellae (see Fig.7).The effect of the microstructure on the crack propagation is studied by comparison of the SEM pictures (all taken after 18,000 load cycles) with the pictures taken periodically with the long distance microscope. Figure 8 illustrates the procedure.

The orientation of most sections of the crack is either 45  or perpendicular to the loading axis. The two dashed circles mark the same section of the zig-zag crack. After 2,000 load cycles a few former pale shades (appeared after 1,000 cycles) became dark lines. These lines propagated during the next 1,000 load cycles, and therefore either they were already real microcracks after 2,000 cycles, or they became real microcracks within the following load cycles. However, in this paper such lines are treated as microcracks, and with this practical simplification the crack propagation curve of the zig-zag crack is given in Figure 9. Figure 9 shows the accumulated crack propagation rate, i.e. the lengths, and the resulting propagation rates, respectively, of all existing sections of the final crack during one scan are summed up. Therefore this diagram of accumulated values represents a kind of averaged crack propagation rate. The typical stop-and-go behaviour of small cracks is observed. The cracks were initiated at grain/phase boundaries (2). Crack stop was caused by pearlite with a comparably high density of cementite lamellae; after changing the direction the cracks continued with intercrystalline propagation. All microcracks (in this case three) coalesced after 7,000 load cycles. The low propagation rate (8) is caused by a pearlitic area with lamellae perpendicular to the crack propagation direction on one side of the crack, i.e. this side is

arrested, and the crack propagates only towards the other side. A similar reason is found for the reduced propagation rate at (10); here one side of the crack has to pass through a field of plastic deformed pearlite whose cementite lamellae lay again nearly perpendicular to the crack path. Finally the crack propagation rate increases steadily after the crack has reached a length of about 75 µm.

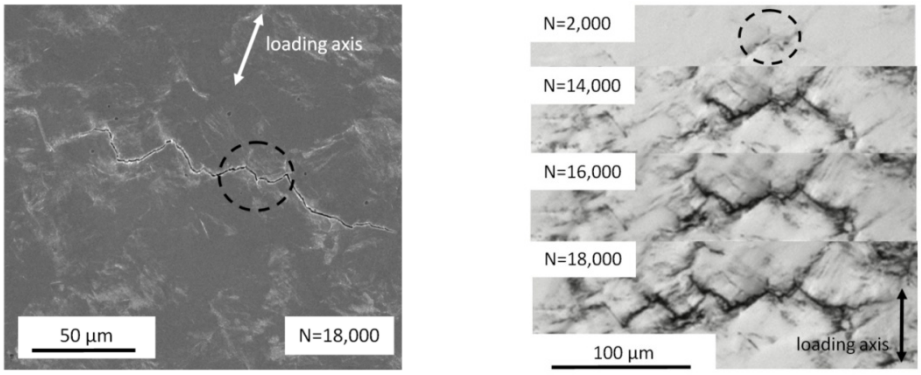


Figure 8. SEM picture (before etching) and optical microscope pictures showing the same zig-zag crack

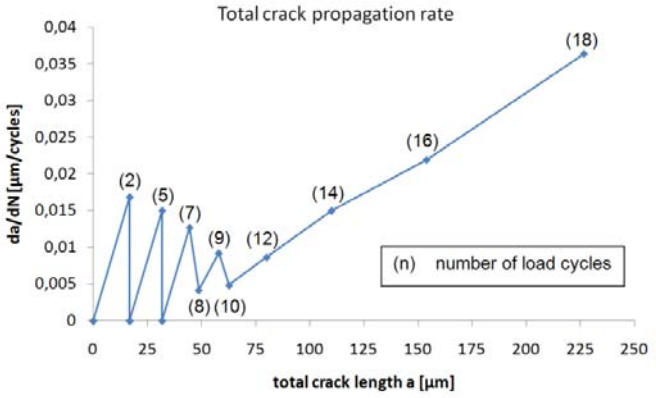


Figure 9. Total crack propagation rate of zig-zag crack

Similar results were found for the other investigated cracks; the propagation rates of all of them increased steadily after they reached a length of about 75 to 100 µm. It was also found that coalescence of microcracks plays an important role. This is a result of the high crack/line-like damage density (see Fig. 6).

The lifetime of the specimens made from the base material can be approximated quite well using a classical fracture mechanics analysis based on long crack data in spite of the complex damage accumulation process described above. This was found out by determining the critical crack size and the lifetime of a long crack located at the notch

root of the hourglass specimen. The starting crack size followed from the threshold value of the da/dN-ΔK-curve, whereas the critical crack was obtained using the value of the fracture toughness obtained with CT-specimens of similar material. Fig. 10 illustrates the procedure. The critical crack size on the specimen surface was determined to be about 2 mm on the basis of the surface topology of the fracture surface (striations in the lower square in Fig. 10 and dimples in the upper square). This value agrees very well with the value of 1.8 mm found in a three dimensional FE-based crack growth simulation program ADAPCRACK3D [3].

The martensite region, on the other hand, showed typical weakest link behaviour under fatigue loading. A minor amount of plastic activity was visible on the surface during testing, but failure was caused by unstable extension of a flaw in the notch root. Careful investigations in the SEM revealed that the fatal flaw was formed in an area containing agglomerates of carbides which apparently had not been dissolved in the heating process. The fracture mechanics analysis based on long crack data revealed that the critical crack size was about 150 µm with the number of load cycles to failure being around 1,000 cycles. The critical crack size agrees well with the fractographic results (s. Fig. 10), whereas the number of load cycles to failure (measured value 48,481) was grossly underestimated. This indicates that the lifetime of the martensite region is initiation dominated. Presumably there are very small micro defects (with sizes of about 1 µm) starting from carbides which have to coalesce in order to form a fracture mechanics defect. Such a mechanism would also explain the large amount of scatter observed as the time to crack initiation depends strongly on the density of undissolved carbides in a specific area. As the density of large carbides is subject to a high degree of local variability in the base material, it is highly likely that this is also true for the undissolved carbides after local heating.

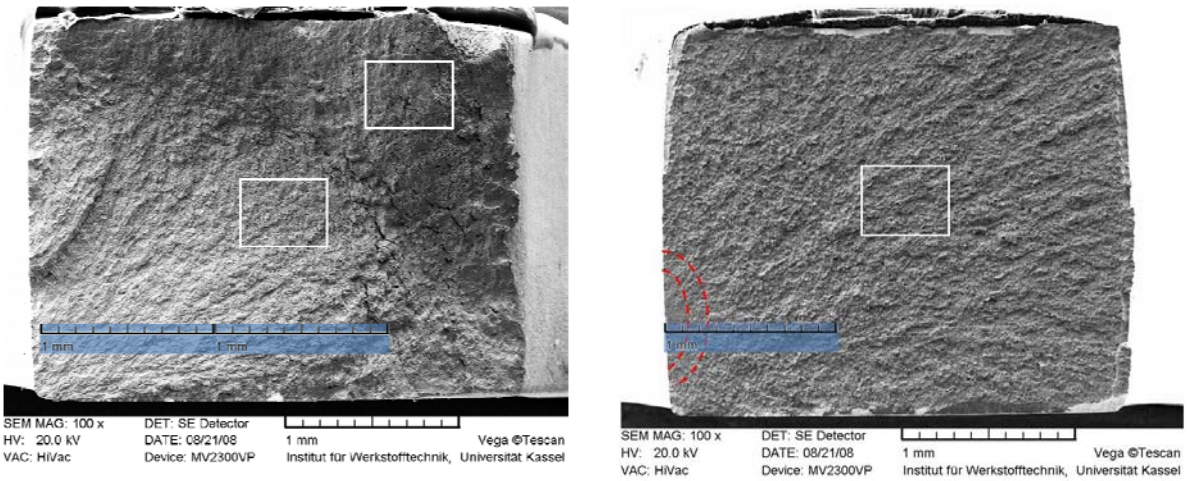


Figure 10. Fracture surface of a specimen cut from the original rod (base material, left side ) and from the outer part of the flange (martensite region, right side)

Specimens taken from the transition zone (specimens number"… -4" and "…-5" in Fig. 3) contain a mixture martensite, bainite and ferrite. The fatigue behavior of the hourglass specimens will depend strongly on the relative location of the notch root and the various kinds of microstructure. This is part of an ongoing research.

## CONCLUSION

The fatigue behaviour of a shaft with local varying microstructure is studied. It is found that the lifetime of specimens taken from the base material (ferrite/pearlite) is well approximated by a classical fracture mechanics analysis, even though multitudinous microcracks are initiated. This implies that the damage accumulation process is growth dominated. On the other hand, regions containing martensite have no visible surface damage during fatigue loading, but fail as soon a crack of some hundred microns is initiated.

## ACKNOWLEDGEMENT

This paper is based on studies carried out by the transregional collaborative research centre SFB/TR TRR 30, which is kindly supported by the German Research Foundation (DFG).

## REFERENCES

1. Weidig U., Huebner K., Steinhoff K. *Bulk steel products with functionally graded properties produced by differential thermo-mechanical processing,* Steel research int 2008; 79 (1): 59-65.
2. Besel M., Brueckner-Foit A. *Surface damage evolution of engineering steel,* Fatigue Fract Engng Mater Struct; accepted for publication 2008.
3. Fulland M., Steigemann M., Richard H.A., Specovius-Neugebauer M. *Numerische Bestimmung des Ermüdungsrisswachstums in inhomogenen Materialien,* DVM-Bericht 240, Zuverlässigkeit von Bauteilen durch bruchmechanische Bewertung: Regelwerke, Anwendungen und Trends, Deutscher Verband für Materialforschung und -prüfung e. V., Berlin, 2008, pp.83-92.
4. Besel M., Brueckner-Foit A., Motoyashiki Y., Schäfer O. *Lifetime distribution of notched components containingvoid defects,* Arch Appl Mech (2006) 76: 645–653